Sustainable Cities and Society 39 (2018) 487–498

Contents lists available at ScienceDirect

Sustainable Cities and Society

journal homepage: www.elsevier.com/locate/scs

Do water bodies play an important role in the relationship between urban form and land surface temperature?

Zhi Cai, Guifeng Han*, Mingchun Chen

College of Architecture and Urban Planning, Key Laboratory of New Technology for Construction of Cities in Mountain Area of Education Ministry, Chongqing University, Chongqing, 400045, China

ARTICLE INFO

Keywords:
Urban form
Land surface temperature
Urban heat island
Water bodies
Cooling effect

ABSTRACT

Water bodies are considered an effective factor in mitigating urban heat island (UHI) effects in large cities. In Chongqing, the largest city in western China, using Landsat 8 data obtained in the daytime during the summer, we analyzed the potential influence of the cooling effects of water bodies on the urban land surface temperature (LST) based on the gradient of the distance to the water bodies (DIST). The results indicate that the cooling effect of water bodies can reach one kilometer (horizontal distance) and have a great impact on the relationship between the urban form factors and LST, particularly at a DIST less than 500 m. The sampling was performed in a 250 m × 250 m grid size, and correlations between four urban form factors (i.e., sky view factor, building density, mean building height and floor area ratio) and the LST gradually increased as the DIST increased. According to the multiple linear regression model, the DIST is an important independent variable at a DIST less than 500 m. This study may help researchers better understand the influence of urban form factors on thermal comfort considering water bodies.

1. Introduction

Due to rapid urbanization, 69% of the global population will live in cities by the end of 2050 (UN-DESA, 2010). The increasing amount and intensity of human activity and the centralization of energy consumption in cities have significantly changed the spatial morphology and energy balance of the original areas, leading to a variety of environmental problems, including the deterioration of the urban thermal environment. Howard (1818) first discovered that the air temperature in urban areas is higher than that in the countryside surrounding London, which is known as an urban heat island (UHI) effect, then the definition of UHI were divided into boundary-layer heat islands, remotely sensed heat islands, surface or subsurface heat islands, daytime heat islands, and non-urban heat islands (Stewart, 2011). Recently, the superposition of the UHI and climate change have caused frequent heat waves in the city (Corburn, 2009). The high temperatures not only exacerbate the circulation of water vapor, resulting in heavy rains, drought and other extreme weather disasters (Fouillet et al., 2006; Ganeshan, Murtugudde, & Imhoff, 2013), but also increase the incidence and mortality of urban diseases. For example, for each 1 °C increase in air temperature above 28 °C, the mortality rate increases by 2% (Chan, Goggins, Kim, & Griffiths, 2012), and higher temperatures lead to increases in air conditioning and refrigeration demand, resulting in a 5–15% increase in electricity consumption (Wong, Jusuf et al., 2011). Therefore, many scholars have paid more attention to UHI mechanisms, influencing factors and mitigation measures and have found that many factors impact UHI, including natural factors (e.g., climate zone and topography) (Chen, Jiang, Tang, & Jia, 2016; Ichinose, Shimodozono, & Hanaki, 1999), physical construction factors (urban form and land use) (Alobaydi, Bakarman, & Obeidat, 2016; Chen, Zhao, Li, & Yin, 2006; Nie & Xu, 2015; Yue, Xu, Tan, Xu, 2007) and immaterial spatial factors (population density and economy patterns) (Santamouris, 2015). Of these influencing factors, urban form/morphology is considered an effective way to reduce the UHI in urban planning (Oke, 1974; Oke, 1987; Taleghani, Kleerekoper, Tenpierik, & Dobbelsteen, 2015).

Urban form refers to the spatial structure and form of urban elements, including land use, transport infrastructure, water and energy infrastructure and the physical form of developments that facilitate human activities and their interactions (Alobaydi et al., 2016; Bokaie, Zarkesh, Arasteh, & Hosseini, 2016; Middel, Häb, Brazel, Martin, & Guhathakurta, 2014). Of these elements, urban fractals, the sprawl index and spatial factors are the main parameters characterizing urban form (Yang, Li, Lin, & Ye, 2011; Zhao, Fu, Liu, & Fu, 2011). Urban form can influence the local urban climate through the form parameters (Stewart & Oke, 2012; Middel et al., 2014). In particular, urban areas with a higher building density and more complex urban morphology

* Corresponding author.
E-mail address: hangf@cqu.edu.cn (G. Han).

https://doi.org/10.1016/j.scs.2018.02.033
Received 12 November 2017; Received in revised form 18 January 2018; Accepted 21 February 2018
Available online 04 March 2018
2210-6707/ © 2018 Elsevier Ltd. All rights reserved.

exhibit more intense heat islands and a lower permeability of urban air ventilation (Chen et al., 2012; Ng, Yuan, Chen, Ren, & Fung, 2011; Xu et al., 2017). On the urban scale, urban form is critical for urban design strategies that can be used to improve the thermal performance conditions in cities (Golany, 1996). However, the application of climate considerations on an urban scale has been limited. Oke (1974) first noted that the UHI was more affected by urban forms, such as land use and building density, on the micro-spatial scale than by those on other scales. Subsequently, many scholars have focused on the relationships between the UHI and other factors, such as the floor area ratio (FAR), mean building height (MH) and sky view factor (SVF) (Chun & Guldmann, 2014; Middel et al., 2014; Schwarz & Manceur, 2014; Taleghani et al., 2015). Chun and Guldmann (2014) explored the potential relationships between the land surface temperature (LST) and five urban characteristics captured over regular grids, i.e., building roof-top areas (BGFA), normal different vegetation index (NDVI), solar radiation (ASR), sky view factor (SVF) and water area, using four statistical models; their results indicated that increasing the BGFA and ASR leads to an increased LST, whereas increasing the NDVI, SVF and water area leads to a decreased LST. Guo, Zhou, Wu, Xiao, and Chen (2016) found that an urban morphology characterized by a medium building height and lower density significantly yielded higher LST variation levels, whereas the lowest LST variation levels occurred in high-rise and high-dense building arrays. Compared to the building height, the building density had a stronger influence on the LST. Medium SVF values produced the lowest LST, whereas the largest and smallest SVF values produced the highest LST. Lee and Oh (2017) found that urban form factors, including the average width of the buildings, average height of the buildings, number of buildings, building surface fraction and terrain roughness class, are statistically correlated with the air temperature, but the correlation coefficients only ranged from 0.32 to 0.54 regardless of whether they were examined during the winter or summer. Of these factors, the building surface fraction is the most positively correlated variable. The relationship between the UHI and urban form varies in different cities due to differences in the climate zone, population, scales and methods (Chen, Zhao, Yao, & Chen, 2016; Takkanon, 2017; Zhang, Murray, & Ii, 2017). To date, conclusive evidence regarding the influences of urban forms or urban structures on the UHI is lacking. The potential quantitative relationships should be examined on micro-meso-macro scales and then used to guide urban planning and construct sustainable and comfortable urban forms.

Recently, heat waves during the summer have become increasingly frequent in cities worldwide; the heat waves also tend to expand more widely and remain in place for a longer time. It is well established that large water bodies, such as oceans, lakes and rivers, have the ability to affect land temperatures by air convection (Coutts, Tapper, Beringer, Loughnan, & Demuzere, 2013; Gunawardena, Wells, & Kershaw, 2017; Moyer & Hawkins, 2017; Theeuwes, Solcerová, & Steeneveld, 2013). The increased surface porosity and bodies of surface water play a role in increasing potential cooling through evaporation. Hathway and Sharples (2012) found significant cooling over a river with an average cooling of nearly 1 °C during ambient conditions greater than 20 °C. Over consecutive hot days in May, substantial cooling occurred over the river, and nearly 2 °C and 1.5 °C cooling occurred on the river bank; the cooling effect of water bodies is significantly affected by the urban form in the surrounding area, including land use types, architectural form, roads, open space and terrain height. The cooling effect of the Ota River in Hiroshima, Japan was found to reach up to 5 °C directly above the river and propagate nearly 100 m from the river banks (Murakawa, Sekine, Narita, & Nishina, 1991). A recent meta-analysis of 27 studies (including remote-sensing based studies) concluded that the water bodies studied could provide a cooling effect of 2.5 K, on average, relative to their context (Gunawardena et al., 2017; Völker, Baumeister, Claßen, Hornberg, & Kistemann, 2013). Water bodies have a greater specific heat capacity than other materials on the land surface; thus, the warming-up speed is slower than that of the surrounding areas, resulting in water bodies that are “cool islands” during the daytime (Oke, 1987; Gunawardena et al., 2017). Through the exchange of air convection, the cooler air on the water bodies blows to the surrounding areas and achieves a cooling effect, and occasionally, this cooling distance can reach one thousand meters (Murakawa et al., 1991). In Japan, cooling from the Ota River was observed to occur close to 300 m from the 270-m-wide river (Murakawa et al., 1991). On a smaller scale, cooling from a 22-m-wide river in Sheffield, UK, was recorded up to 30 m from the river banks (Hathway and Sharples, 2012). Theeuwes et al. (2013) constructed a mesoscale model of hypothetical water bodies simulated within an idealized city. Their study highlighted that relatively large water bodies have the greatest cooling effect in areas adjacent to their boundaries and downwind areas. The size and length of the downwind spread depend on the wind velocity, and relatively cooler air originating from a large urban water body is transported by wind to generate plumes several kilometers long.

However, using air temperature to identify the cooling effect of water bodies is limited because most air temperature measures rely on measured or local weather station data. Meeting the high spatial resolution requirements of temperature on an urban scale and considering the influence of water forms or urban forms on the cooling effect of water bodies is challenging using these data. Furthermore, many studies have noted that the LST and air temperature are closely related and have similar spatial patterns (Klok, Zwart, Verhagen, & Mauri, 2012; Nichol, Fung, Lam, & Wong, 2009). Therefore, LST data retrieved from remote sensing images or urban climate models are widely used by scholars to study the urban thermal environment, particularly urban form/morphology (Sun, 2012; Sun, Chen, Chen, & Lü, 2012). These authors have found that the cooling effectiveness (magnitude and distribution) of water bodies is influenced (inter alia) by the size, shape and spread of such spaces and the distance among them (Sun, 2012). Du et al. (2016) found that the cooling of water bodies can vary depending on their geometry, with lakes demonstrating larger cooling effects than rivers. Any benefits of the river are lost quickly where the site is physically cut off from the water by walls or buildings. Sun (2012) and Syafii et al. (2017) found that water bodies with a large area and regular shape have a better cooling effect than other water bodies. Sun et al. (2012) found that the shape and location are significant indicators influencing the cooling effect of wetlands (i.e., reservoirs, lakes and rivers) in an urban region. Theeuwes et al. (2013) confirmed a previous remote-sensing study that suggested that several smaller, regularly shaped water bodies distributed equally within an urban area generate smaller temperature effects (particularly during the day) than a single larger water body with a similar total volume. Although the studies discussed above provide evidence of the heat transfer between water sources and the environment and support the methods of modeling this behavior (Huang, Zhao, Wang, Zhu, & Li, 2008; Hannah, Malcolm, Chris, & Youngson, 2010; Kim et al., 2008), these studies do not provide direct evidence of the provision of cooling in a complex urban environment (Hathway & Sharples, 2012).

Although several urban planners and architects have used water bodies as planning and design tools to mitigate the UHI and improve the living environments in cities (Coutts et al., 2013; Hathway & Sharples, 2012; Steeneveld, Koopmans, Heusinkveld, & Theeuwes, 2014; Xu et al., 2017), previous studies have not focused on the effect of specific urban forms in the river corridor and the propagation of cooling from rivers to urban environments (Hathway & Sharples, 2012). Therefore, exploring the interaction between the cooling effect of water bodies and the urban form in the surrounding area is necessary to improve the synergistic cooling potential.

The goal of this study is to evaluate the relationships between urban form factors and the LST near rivers after considering the influence of the river’s cooling effect. This paper aims to

1) find what is the effect of water bodies on the LST;
2) determine whether the effect of water bodies can change the

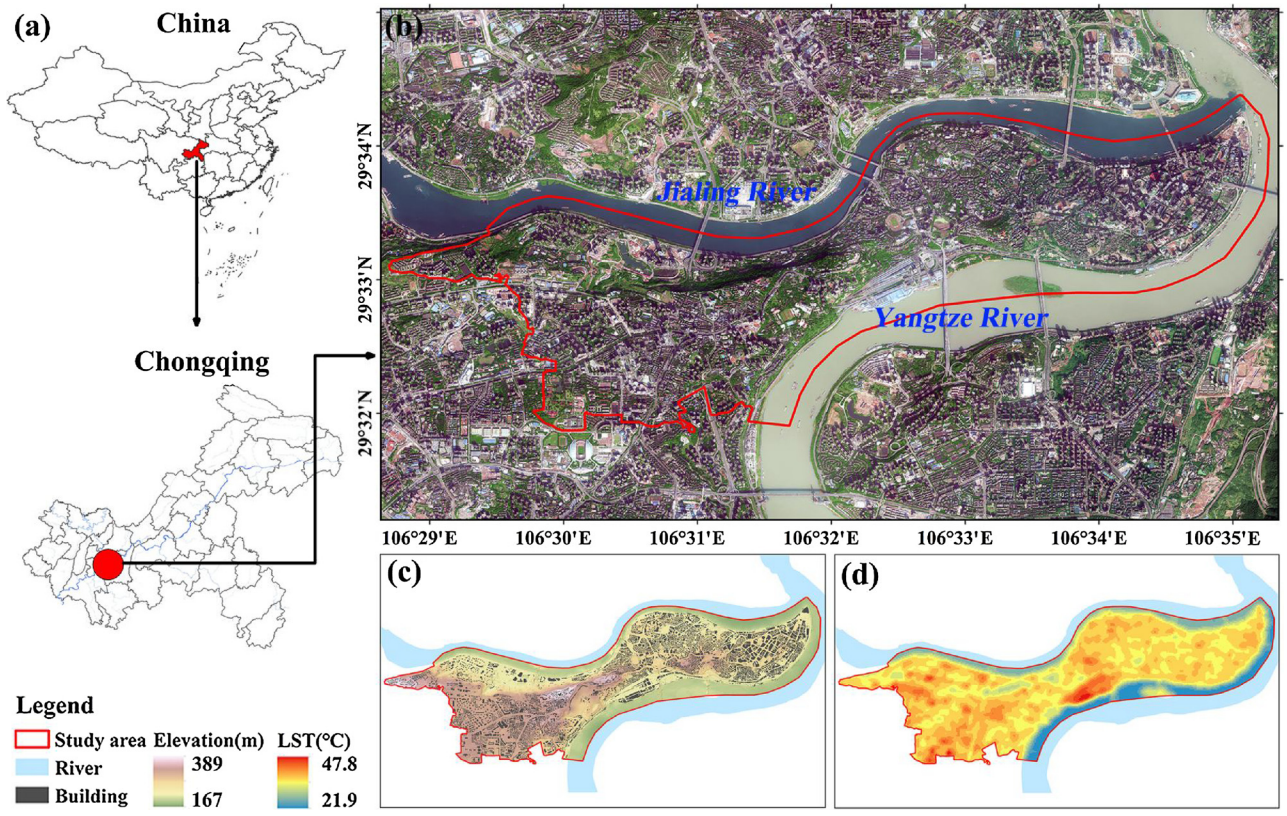


Fig. 1. (a) Location; (b) Yuzhong district and study area; (c) Elevation and the distribution of building; (d) Spatial distribution of LST retrieved from Landsat 8.

relationship between urban form factors and the LST; and

3) reveal a potential quantitative correlation between urban form factors and the LST by including both urban form factors and distance from water bodies in a linear regression model.

2. Data and methods

2.1. Study area

Yuzhong district is an original area in Chongqing City located within the range of 29°31′50″–29°34′20″N and 106°28′50″–106°35′10″E and beyond the subtropical monsoon climate zones; this district is situated in the peninsula formed by the intersection of the Yangtze River, which is the largest river in China, and its branch, the Jialing River, in an 18.54 square kilometer land area (Fig. 1b). There is a great fluctuation in the topography, with a maximum difference of 227 m (Fig. 1c). The climate is characterized as a typical hot and humid climate influenced by a mountainous terrain and two large river bodies, and the static wind frequency is up to 50% throughout the year with average wind speeds of less than three meters per second (Yong, Wen, & Zhao, 2004); the average humidity is above 70%. The study area is dominated by compact high-rise buildings with few green spaces and contains 970.10^3 people, with an average population density of 52.10^3 people per square kilometer. The UHI effect is very serious due to the high population and building density. According to the historical meteorological data, the heat island effect in Chongqing City has increased by 0.036 °C annually, the temperature is above 35 °C on 15–25 days during the summer, and the maximum temperature can reach 44 °C (Li & Yu, 2014).

2.2. Data sources and processing

2.2.1. Data sources and pre-processing

Landsat 8 remote sensing images acquired on July 10, 2016 11:27 AM with no cloud coverage above the study areas were downloaded from the website (http://www.gscloud.cn) and used in this study. Landsat 8 TIRS Band 10 (the thermal infrared band) data with a spatial resolution of 100 m (resampled to 30 m to match the multispectral bands) were used to retrieve the LST by ENVI 5.1 software (Table 1). The Landsat 8 OLI Band 4 (red band) and band 5 (near-infrared band) were used to extract the normal difference vegetation index (NDVI), which was converted into green coverage, excluding non-vegetation areas with an NDVI less than 0. The other data included demographic data of the communities and management grids in 2014 collected from the Statistics Bureau of Yuzhong District. The current land use map (2014), construction map (2014), and regulatory plans (2010) covering the entire district were collected from the Department of Housing and Urban-Rural Development of the Yuzhong government. The digital elevation model (DEM) was created from digital topographic maps on a scale of 1:500.

2.2.2. Retrieved land surface temperature

ENVI 5.1 software was used to preprocess the raw images, including the radiometric calibration, atmospheric correction and cutting. For the atmospheric correction, the atmospheric radiation process was simulated using the atmospheric correction MODTRAN model, which is based on the radiative transfer equation (RTE). Using the simulation, the atmospheric downward radiance L↓, upward radiance L↑, and

Table 1
Parameters of Landsat 8.

Sensor	OLI		TIRS
Band	Band 4 Red	Band 5 NIR	Band 10 TIRS
Resolution (m)	30	30	100
Resample resolution (m)	30	30	30
Wavelength (μm)	0.636–0.673	0.851–0.879	10.60–11.19

transmissivity τ can be obtained from the NASA website (http://atmcorr.gsfc.nasa.gov/).

$$L_{sensor} = [\varepsilon B(T_S) + (1 - \varepsilon)L\downarrow]\tau + L\uparrow$$

L_{sensor} is the radiation intensity ($W\,m^{-2}\,sr^{-1}\,\mu m^{-1}$) of wave band 10 measured by satellite sensor. L_{sensor} can be obtained by the gray value of the raw images according to

$$L_{sensor} = gain \times Qcal + offset$$

Qcal is the gray value, *gain* is the gain value in wave band 10, and *offset* is the deviation value in wave band 10. For the two thermal infrared bands of Landsat 8 TIRS, both the gains (0.0003342) and offsets (0.1) are identical.

ε is the land surface emissivity; the OLI Band 10 has a similar spectral range to TM and the ETM ± thermal infrared band; thus, we used the NDVI threshold method (Sobrino, Jiménez-Muñoz, & Paolini, 2004) to calculate the land surface emissivity. The formula is as follows:

$$\varepsilon_{water} = 0.995$$

$$\varepsilon_{surface} = 0.9265 + 0.0614P_V - 0.0461P_V^2$$

$$\varepsilon_{building} = 0.9589 + 0.086P_V - 0.0671P_V^2$$

where ε_{water} is the water surface emissivity, and $\varepsilon_{surface}$ is the natural surface emissivity (e.g., grassland, arable land and sparse vegetation cover). $\varepsilon_{building}$ is the built-up surface emissivity. P_v is the vegetation fraction and can be calculated using the following formula:

$$P_V = \frac{NDVI - NDVI_{soil}}{NDVI_{veg} - NDVI_{soil}}$$

NDVI is the normalized difference vegetation index, $NDVI_{soil}$ is the value of the completely bare soil or non-vegetation area, and $NDVI_{veg}$ is the value of an area that is fully covered by vegetation. Empirically, $NDVI_{soil}$ is 0.05, and $NDVI_{veg}$ is 0.7. When $NDVI > 0.7$, the value of P_v is 1, but when $NDVI < 0.05$, P_v is 0. NDVI can be calculated using the following formula:

$$NDVI = \frac{NIR - R}{NIR + R}$$

For Landsat 8 OLI, NIR is band 5 (near-infrared band), and R is band 4 (red band).

$B(T_s)$ is the black body radiance. The radiant brightness of the black body in the thermal infrared band can be expressed as follows:

$$B(T_s) = \frac{C_1}{\lambda^5(e^{C_2/\lambda T_s} - 1)}$$

C_1 and C_2 are radiation constants with values of $1.19104356 \times 10^8\,W m^{-2}\,sr^{-1}\,\mu m^4$ and $1.4387685 \times 10^4\,\mu m\,K$, respectively, and λ is the wavelength (μm). $B(T_S)$ can be transferred as follows:

$$T_S = \frac{K_2}{\ln(K_1/B(T_S) + 1)}$$

For the Landsat 8 TIRS Band 10 data, $K_1 = 774.89\ W m^{-2}\,sr^{-1}\,\mu m^{-1}$ and $K_2 = 1321.08\ K$.

2.2.3. Selected urban form factors

In this study, we selected the following four urban form factors based on the Local Climate Zones (LCZ) scheme categories (Stewart & Oke, 2012): building density (BD), sky view factor (SVF), mean building height (MH) and floor area ratio (FAR) (Table 2). In addition, NDVI is used as a common index of green coverage.

2.3. Methodology

2.3.1. Stepwise sampling

In studies exploring the urban environment, the spatial scale (grid size) is an important variable that can play a decisive role. Due to the complex surface composition and buildings in urban areas, data sampled on grid sizes that are too small may fail to represent the whole area; additionally, if the data are sampled on grid sizes that are too large, detailed information may be ignored, leading to a low resolution. Based on previous relevant studies (Han, Cai, Xie, & Zeng, 2016; Masson et al., 2014; Nassar, Blackburn, & Whyatt, 2016), we selected a grid size of 250 m × 250 m as an appropriate spatial scale for this study area using Landsat images. Considering the cooling effect of water bodies and its potential maximum cooling distance (Theeuwes et al., 2013), we used a stepwise sampling method in which we gradually removed the samples near the water bodies, and the remaining cells (pixels) were used to analyze the correlation between the LST and urban factors, to find whether the LST increases with distance and whether the correlation between the urban form factors and the LST changes depending on the distance. The step length is 250 m; thus, as the distance to the water bodies (DIST) increases by 250 m, the samples covered by the distance are removed. The farther the distance, the fewer remaining sample used in the analysis (Fig. 2). The average urban form factors and the LST at each step were extracted using the spatial analyst tools in ArcGIS 10.2.

2.3.2. Pearson correlation and regression analysis

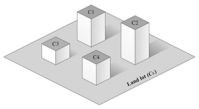
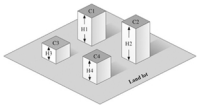
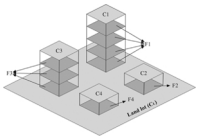
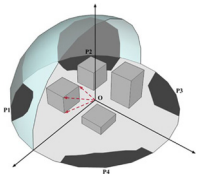
The Pearson correlations between each urban form factor and the LST were analyzed using SPSS (version 24.0) software. Using a stepwise regression method (after removing the strong interaction parameters), a multiple linear regression model was established between the LST as the dependent variable and the urban form factors as the independent variables based on the ordinary least squares (OLS), which illuminate the combined impact effects of the urban form factors on the urban surface heat island effects. Standardized regression coefficients were also used to explain and compare the degree of influence of each factor. Comparing the Pearson correlation coefficients and the value of R squared using the F-statistics of the multiple linear regression on each spatial scale, we attempted to find whether the cooling effects of the water bodies change the correlation relationships between the urban form factors and the LST and reveal how far the cooling effects of the water bodies can reach in the surrounding area.

3. Results

3.1. Correlations between urban form factors and DIST

The results calculated using SPSS software showed that the DIST is significantly positively correlated with the LST when the DIST is less than 1 km (Fig. 3). Thus, the LST increases as the DIST increases, and the surrounding area near the water bodies has a lower LST than the farther areas. Water bodies have a larger specific heat capacity and can be cooled through evaporation; the heating rate of water bodies is much slower than that of land surfaces. Through the process of energy transfer and heat exchange by air, water bodies can achieve a significant cooling effect on the surrounding land surface. The DIST is significantly positively correlated with the SVF and NDVI, whereas the DIST is significantly negatively correlated with the BD, MH and FAR. Thus, the number of green spaces increases as the DIST increases, and the area near the water bodies have more building construction than farther areas. Notably, the Pearson correlation coefficients and their significances were tested by performing t-statistics and increased as the DIST increased. The correlation coefficients and optimal cubic fitting functions indicate that the cooling effect of the water bodies is limited, which is consistent with many previous studies (Du et al., 2016; Sun et al., 2012). The maximum cooling distance of water bodies is obtained by seeking the inflection point of the cubic function (Fig. 4). We found that the cooling distance ($\Delta DIST_{max}$) is 945 m and that the maximum cooling effect (ΔT_{max}) is 4.75 °C. The study area is a narrow peninsula in the east-west direction; its narrowest width is only 1.1 km, and its

Table 2
Urban form factors.

Urban form factors	Definition	Formula	Illustrate
Building Density	The percentage of land surface covered by buildings in a land lot.	$BD = \frac{\sum_{N}^{i=1} C_i}{C_L}$ C_i is the coverage area of the building; C_L is the area of the land lot.	
Mean Building Height	Mean building height in a land lot.	$MH = \frac{\sum_{N}^{i=1} C_i H_i}{\sum_{N}^{i=1} C_i}$ C_i is the coverage area of the building; H_i is the building height.	
Floor Area Ratio	The ratio of the total floor area to the land area of a land lot.	$FAR = \frac{\sum_{N}^{i=1} C_i F_i}{C_L}$ C_i is the coverage area of the building, F_i is the number of building floors, and C_L is the area of the land lot.	
Sky View Factor	The ratio between the radiation received by a planar surface and the entire hemispheric radiating environment (Watson & Johnson, 1987).	$SVF = 1 - \sum_{N}^{i=1} \sin^2\beta_i\left(\frac{\alpha_i}{360°}\right)$ N is the total number of the angle elements of the obstacles in the hemispheric environment; and α_i and β_i reflect the elevation and azimuth angles of the angle element i, respectively. (Matuschek & Matzarakis, 2010)	

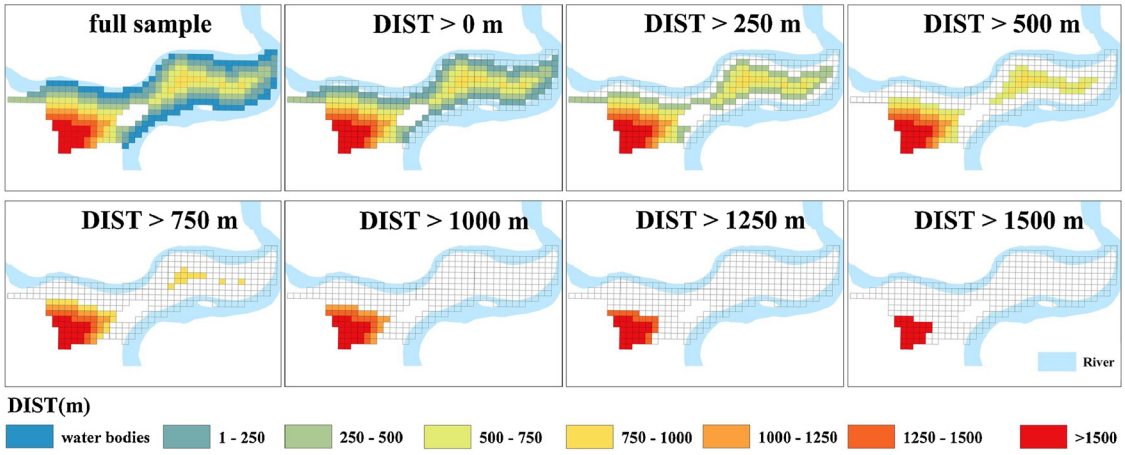


Fig. 2. Stepwise sampling according to the DIST.

widest width is 2.1 km, indicating that most of the region of the study area may be under the influence of the water bodies' cooling effect.

3.2. Influence of water bodies' cooling effect on the correlation between the urban form factors and the LST

According to the Pearson correlation coefficients between the urban form factors and the LST, the correlations remained low and stable when the DIST was less than 500 m (0 m < DIST ≤ 500 m); however, when the DIST was more than 500 m (DIST > 500 m), the correlations between the LST and certain urban form factors (i.e., SVF, MH, and FAR) increased rapidly (Fig. 5). By comparing the scatter plots before and after the removal of the influenced samples (Table 3), the water bodies were found to have a great impact on the relationship between the urban factors and the LST, particularly when the DIST was less than 250 m (0 m < DIST ≤ 250 m), and a stronger influence can change the correct relationship between the urban form factors and LST. As shown in Tab 3, no stable or weak linear regression models were observed between the urban form factors and LST as a DIST less than 250 m (0 m < DIST ≤ 250 m), but after gradually removing the samples under the influence of the water bodies, the linear regression models between the urban form factors and the LST become more significant.

The SVF was significantly positively correlated with the LST, but a weak correlation was observed without considering the influence of the water bodies (Fig. 5). For example, using all samples to calculate the correlation, the correlation coefficient between the SVF and LST is only 0.254 ($P < 0.01$), indicating that the cooling effect of the water bodies is not considered (DIST > 0 m). After removing samples less than 250 m from the water bodies, the Pearson correlation coefficients were also only 0.273 ($P < 0.01$). However, after removing samples with DIST less than 500 m, the Pearson correlation coefficient calculated using samples with a distance greater than 500 m rapidly increased to 0.462 ($P < 0.01$) and remained stable as the distance continued to increase. As a main factor reflecting the open space and efficacy of shielding, a higher SVF always indicates fewer buildings or a low-rise urban form in which a large amount of solar radiation can reach the land surface; thus, a higher SVF can lead to a higher LST during the daytime. However, by comparing the spatial distribution of the samples, i.e., the LST and SVF values at each distance gradient, we found that most samples with large SVF values and low LST values are distributed in the area near the water bodies (Table 3). Thus, the open areas are more susceptible to water bodies. An open space or ventilation

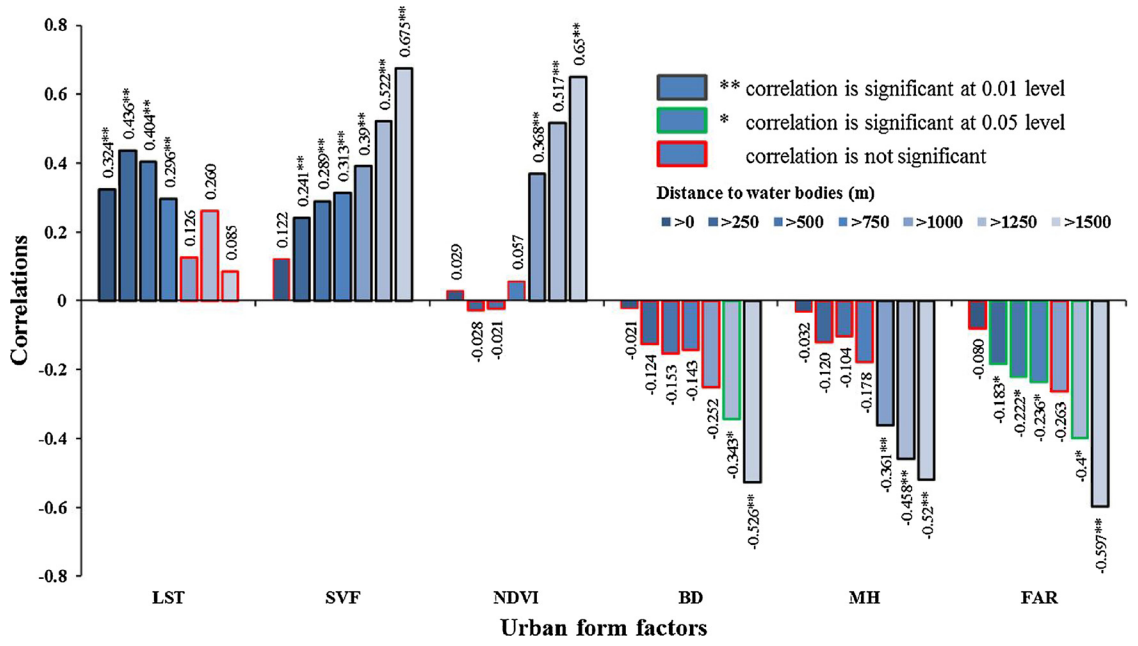


Fig. 3. The Pearson correlation coefficients between the DIST and urban form factors.

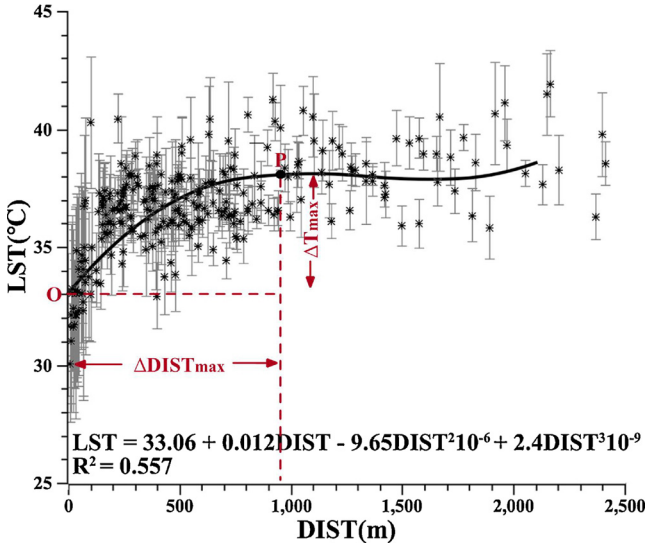


Fig. 4. Scatter plots of the DIST (DIST > 0 m) and LST on a distance gradient.

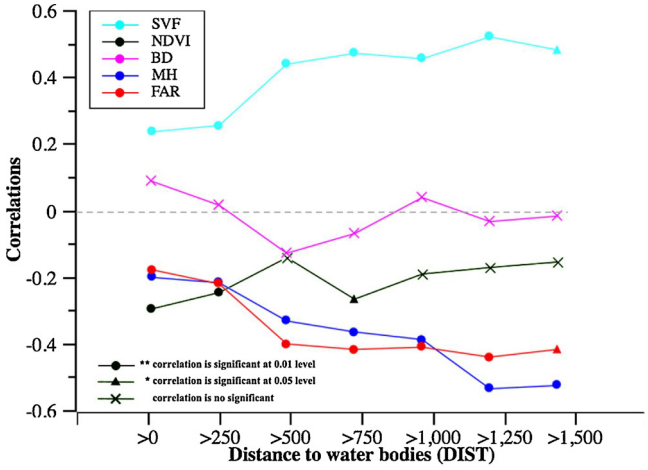


Fig. 5. The Pearson correlation coefficients between the urban form factors and LST as the DIST increased.

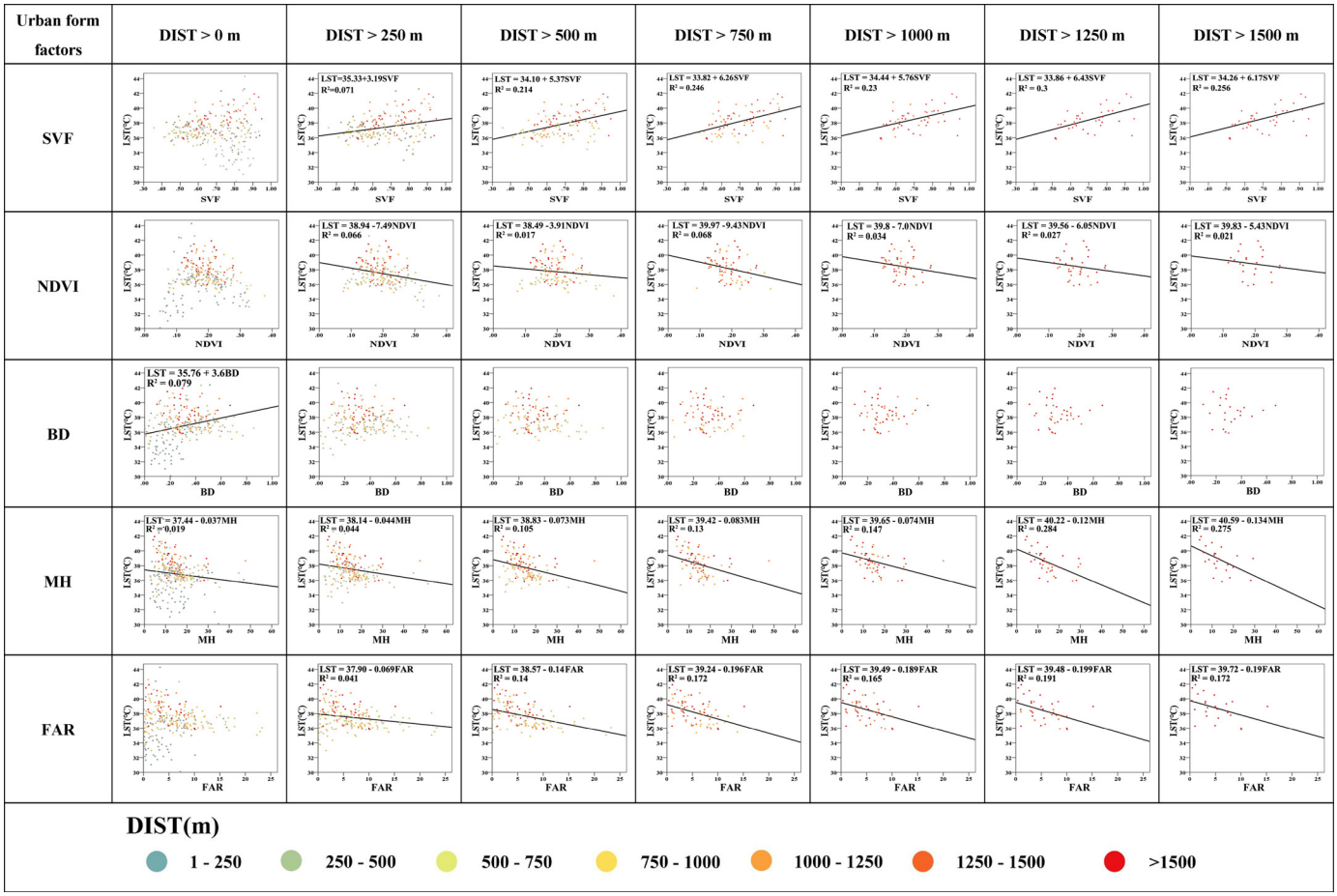
corridor is beneficial to air flow and accelerates the exchange of heat, resulting in a significant cooling effect on the land surface, which weakens the positive relationship between the SVF and LST. As the DIST increases, the cold air flow from the water bodies is gradually heated by the land surface or buildings, and its cooling effect decreases, weakening the effect of the water bodies on the farther area, and the positive correlation between the SVF and LST becomes stronger.

As a common index of green coverage, the NDVI was significantly negatively correlated with the LST. The Pearson correlation coefficient decreased as the DIST increased (Fig. 5). However, according to the linear regression models, NDVI had insufficient power to explain the LST using all samples (DIST > 0 m) (Table 3). However, after removing samples with a DIST less than 250 m, the linear regression models between the NDVI and LST immediately became significant. The scatter plots also indicated that the samples near the river bodies had low LST values (Table 3), indicating that the water bodies had a great impact on the surrounding area and interfered with the correct quantitative relationship between the NDVI and LST.

The BD was not significantly correlated with the LST. However, the correlation between the LST and BD can be predicted by a linear regression model in DIST > 0 m, but the R square is only 0.079. The scatter plots indicated that the samples with the lowest BD values and LST values were near the water bodies (Table 3). Thus, lower BD areas are easily affected by the cooling effect of water bodies, resulting in a general weak positive correlation between the LST and BD. After gradually removing the samples under the cooling effect of the water bodies by stepwise sampling, the positive correlation immediately disappeared.

The MH and FAR are both significantly negatively correlated with the LST, which is consistent with the findings reported by Lin, Siu, Qin, and Gou (2017). The higher MH and FAR values indicate the presence of a high-rise urban form and large amount of shadows provided by high buildings, which greatly reduce the amount of solar radiation that reaches the land surface, resulting in a lower LST. Theoretically, the lower the MH or FAR values, the higher the LST during the daytime. However, according to the scatter plots, a large number of samples near water bodies had low LST, MH and FAR (Table 3), indicating that the cooling effect of the water bodies has a great impact on the relationship

Table 3
Scatter plots of the urban form factors and the LST of each distance gradient.



among the LST, MH and FAR on the surrounding area. Compared to samples with low LST values, in certain samples from the same area near the water bodies that had high LST, MH and FAR values (Table 3), we found that the low-rise area is easily affected by the cooling effect of the water bodies. The cooling effect of the water bodies is achieved by air convection, and a "wall" can easily be formed by tall buildings (Wong, Nichol, & Ng, 2011), preventing air convection and reducing the cooling effect of the water bodies. After gradually removing the samples near the water bodies, the negative correlation between the LST, MH and FAR became stronger.

3.3. Combined impact of urban form factors on the LST

The linear regression models (Table 3) indicate that significant linear relationships exist between the LST as the dependent variable and the SVF, NDVI, MH and FAR as single independent variables. However, the linear relationships between the LST and single urban form factors remained weak because the R-squared values only ranged from 0.105 to 0.214, even though the regression models tested by the F-test and coefficients tested by the *t*-test (two-tailed) are all significant. Thus, any single urban form factor and any single model cannot predict the land surface temperature or land surface urban heat island.

To further determine the impact of the water bodies and reveal the potential quantitative correlation between the urban form factors and LST, a multiple stepwise regression model (in which the strong interaction parameters were removed at each DIST) is established between the urban form factors and the LST to better understand the combined impact of the urban form factors on the land surface thermal environment (Table 4). The LST is the dependent variable, and the urban form factors and DIST are the independent variables. Table 4 shows that the DIST acts as a main independent variable in samples with a distance to the water bodies less than 500 m (DIST > 0 m and DIST > 250 m) and that the stronger cooling effect of the water bodies resulted in insignificant correlations between certain urban form factors (SVF, NDVI and MH) and the LST (DIST > 0 m). However, as the DIST increased, the cooling effect of the water bodies weakened, and the other urban form factors began to exert a greater influence on the LST. The regression model improved markedly as the DIST increased. In addition, the R-squared ranged from 0.360 to 0.518, but the prediction ability of the regression model remained insufficient.

Clearly, the linear regression models have an insufficient capacity to predict the LST using the urban form factors. Two reasons may explain these results. First, other urban form factors are not considered. Second, according to previous studies, the impact of the urban form factors on the LST is a nonlinear process as follows: the cooling effect of the water bodies depends nonlinearly on the fractional water cover, size, and distribution of individual lakes within the city with respect to the wind direction (Theeuwes et al., 2013).

4. Discussion

4.1. The influence of water bodies on the urban thermal environment

Notably, water bodies have an influence on the urban thermal environment, particularly in cities with larger water bodies. We found that the cooling effect of water bodies has a great impact on the

Table 4
Regression analysis results.

	DIST > 0m				
Model	U.C.	S.C.	t	Sig.	VIF
(Constant)	38.884		161.938	0.000	–
SVF	–	–	–	–	–
NDVI	–	–	–	–	–
BD	9.178	0.736	8.870	0.000	2.921
MH	–	–	–	–	–
FAR	−0.225	−0.493	−5.970	0.000	2.887
DIST	0.001	0.341	6.916	0.000	1.029
N = 272.					
Adj. R^2 = 0.360, S.E. of regression = 1.67.					
F-statistic = 51.901, Prob (F-statistics) = 0.000.					
	DIST > 250 m				
Model	U.C.	S.C.	t	Sig.	VIF
(Constant)	44.991		63.026	0.000	–
SVF	[a]	–	–	–	–
NDVI	−14.87	−0.563	−6.990	0.000	1.991
BD	3.995	0.435	4.112	0.000	3.438
MH	−0.045	−0.223	−2.584	0.011	2.293
FAR	−0.194	−0.608	−4.750	0.000	5.033
DIST	0.0004	0.140	2.373	0.019	1.071
N = 196.					
Adj. R^2 = 0.366, S.E. of regression = 1.22.					
F-statistic = 23.472, Prob (F-statistics) = 0.000.					
	DIST > 500 m				
Model	U.C.	S.C.	t	Sig.	VIF
(Constant)	45.561		61.496	0.000	–
SVF	[a]	–	–	–	–
NDVI	−13.63	−0.528	−5.795	0.000	1.787
BD	4.306	0.487	4.027	0.000	3.151
MH	−0.049	−0.239	−2.393	0.018	2.145
FAR	−00254	−0.797	−5.582	0.000	4.389
DIST	–	–	–	–	–
N = 129.					
Adj. R^2 = 0.405, S.E. of regression = 1.09.					
F-statistic = 22.798, Prob (F-statistics) = 0.000.					
	DIST > 750 m				
Model	U.C.	S.C.	t	Sig.	VIF
(Constant)	38.496		20.989	0.000	–
SVF	7.213	0.621	4.866	0.000	2.399
NDVI	−10.27	−0.324	−3.343	0.001	1.380
BD	5.418	0.489	3.875	0.000	2.343
MH	−0.065	−0.307	−3.106	0.003	1.439
FAR	[a]	–	–	–	–
DIST	–	–	–	–	–
N = 77.					
Adj. R^2 = 0.483, S.E. of regression = 1.05.					
F-statistic = 18.784, Prob (F-statistics) = 0.000.					
	DIST > 1000 m				
Model	U.C.	S.C.	t	Sig.	VIF
(Constant)	34.892		18.617	0.000	–
SVF	8.336	0.671	4.628	0.000	1.913
NDVI	[a]	–	–	–	–
BD	7.262	0.576	4.268	0.000	1.656
MH	−0.043	−0.215	−1.824	0.074	1.261
FAR	[a]	–	–	–	–
DIST	–	–	–	–	–
N = 51.					
Adj. R^2 = 0.450, S.E. of regression = 1.12.					
F-statistic = 14.659, Prob (F-statistics) = 0.000.					

(*continued on next page*)

Table 4 (*continued*)

	DIST > 1250 m				
Model	U.C.	S.C.	t	Sig.	VIF
(Constant)	38.429		14.644	0.000	–
SVF	7.546	0.618	3.461	0.002	2.384
NDVI	−10.29	−0.269	−2.127	0.041	1.197
BD	5.480	0.410	2.712	0.011	1.703
MH	−0.085	−0.360	−2.362	0.024	1.735
FAR	[a]	–	–	–	–
DIST	–	–	–	–	–
N = 37.					
Adj. R^2 = 0.518, S.E. of regression = 1.11.					
F-statistic = 10.670, Prob (F-statistics) = 0.000.					
	DIST > 1500 m				
Model	U.C.	S.C.	t	Sig.	VIF
(Constant)	36.457		13.566	0.000	–
SVF	13.430	1.113	5.048	0.000	2.222
NDVI	[a]	–	–	–	–
BD	5.804	0.450	2.355	0.029	1.672
MH	[a]	–	–	–	–
FAR	[a]	–	–	–	–
DIST	–	–	–	–	–
N = 24.					
Adj. R^2 = 0.497, S.E. of regression = 1.19.					
F-statistic = 8.560, Prob (F-statistics) = 0.000.					

U.C. denotes unstandardized coefficient.
S.C. denotes standardized coefficient.
[a] The strong interaction parameters were removed.

correlation between the urban form factors and the LST in Chongqing City in the daytime during the summer. Using the full sampling method to study the relationship between the urban form factors and the LST, the strong positive correlation between the LST and NDVI appears highly abnormal as shown in Fig. 6, but we found that most abnormal samples are water bodies (NDVI < 0) or the samples under the cooling effect of water bodies (0 < NDVI < 0.1 and LST < 35 °C). Previous studies have also shown the abnormal correlation between the urban form factors and the LST and demonstrated that water bodies have an influence on the urban thermal environment. Guo et al. (2015) used summer daytime data to study the urban biophysical composition of land surface temperatures in urban heat island clusters and found that the strong negative liner relationship between the LST and NDVI only existed when the NDVI values were greater than approximately −0.06, but it is difficult to explain the abnormal scatter plots at NDVI values less than −0.06. However, this relationship can be explained by considering the water bodies and including the water bodies as samples when NDVI values less than −0.06. Zhang, Estoque and Murayama (2017) used LST data to study the UHI effect in Nanchang City and found an unusual correlation between the LST and NDVI. There existing a larger number of abnormal scatter plots (NDVI < 0.5 and LST < 26 °C) similar as we have found in Chongqing City, and the similar results were also obtained by Chen and Zhang (2017) and Xu and Chen (2017).

4.2. The influence of the sampling method and land use on the studies of urban thermal environment

As statistical data which based on samples are widely used in urban thermal environment studies, that the sampling method (i.e., random sampling, full sampling, sampling along the straight-line and sampling along the road) should be carefully designed and to avoid statistic error. Although most of the scholars has taken a careful design about the sampling method before conducting the study, such as using the random sampling method to avoid the spatial autocorrelation and adopting equidistant sampling method to fulfill the equilibrium of spatial distribution. It should be noticed that these methods cannot avoid the potential influence of green spaces, water bodies, corridor and other factors on its results, especially in studies using few samples in which the data were measured or a random sampling method was used; abnormal samples or plots may significantly interfere with the quantitative relationship between the urban form factors and LST and lead to an incorrect conclusion. With the influence of water bodies as an example, if inappropriate samples and data are used, the scatter plots may appear as those shown Fig. 7. Fig. 7c and e in which many samples near water bodies and few samples far from water bodies are used; this "smile" curve or negative relationship most likely occurs when a large river passes through a city. In addition, a well-designed sampling method may help improve the reliability of a study and show a stronger correlation between the urban form factors and LST (Fig. 7d).

Considering the difference in the land use and impervious materials and their impact on the relationship between the urban form factors

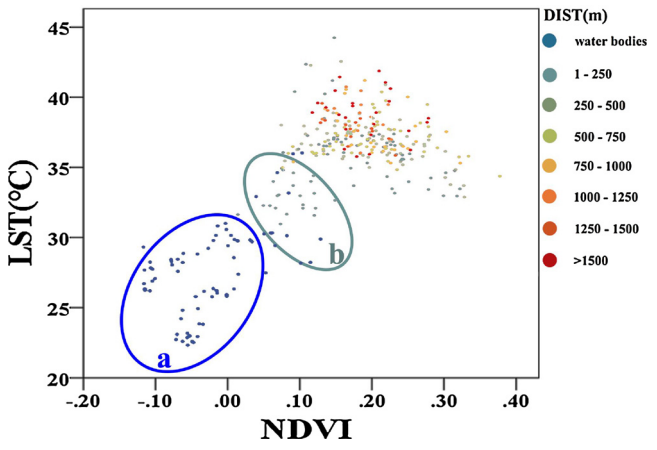


Fig. 6. Relationship between the NDVI and LST; (a) Water bodies; (b) Samples under the influence of water bodies.

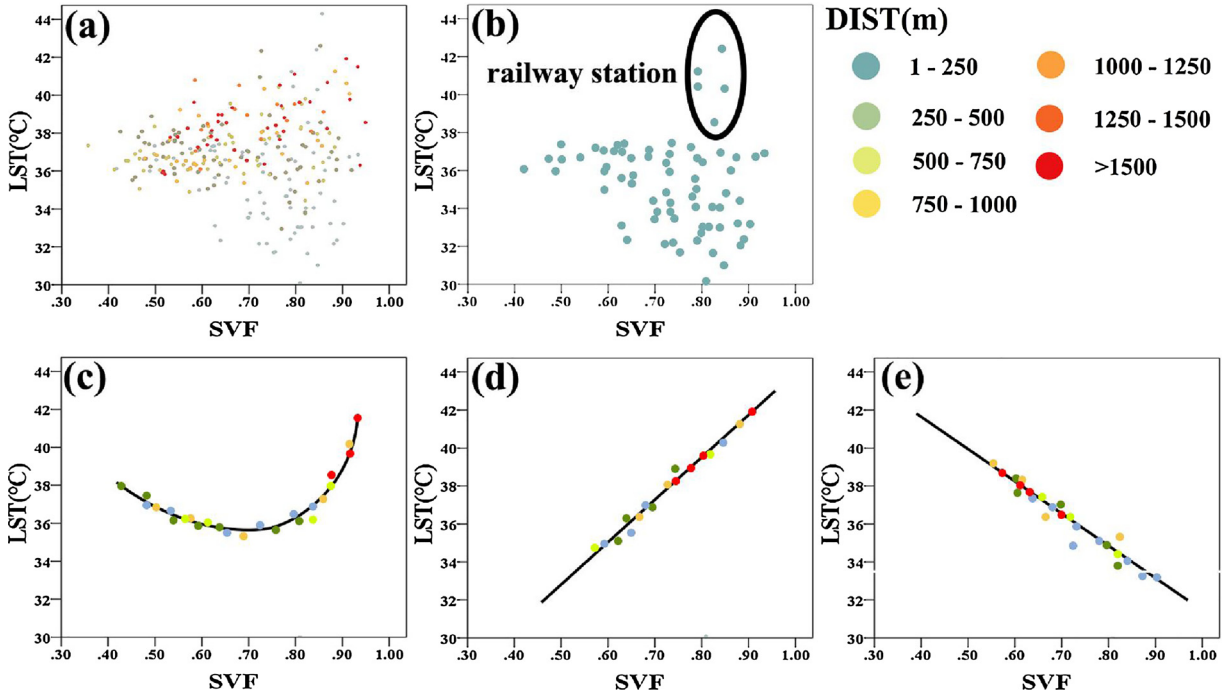


Fig. 7. Relationship between SVF and LST; (a) Full sampling and excluding water body samples; (b) Samples where 0 < DIST < 250; (c) "smile" curve relationship between SVF and LST; (d) Stronger positive relationship between SVF and LST; (e) Stronger negative relationship between SVF and LST.

and the LST is necessary. As shown in Fig. 7b, the samples with the highest SVF values and LST values near water bodies are railway stations because darker iron materials and high anthropogenic heat release cause higher LSTs. The rooftop materials of buildings in urban villages may also lead to an extraordinary relationship between the urban form factors and LST as found by Guo et al. (2016) in Guangzhou city, China. In addition, a refined urban form/morphology classification scheme, such as local climate zones (Stewart & Oke, 2012), may clarify the correlation between the urban form factors and LST under different site conditions.

5. Conclusion

Water bodies have an obvious impact on the relationships between the urban form factors and the LST, particularly at a DIST less than 250 m. The water bodies even change the correlations between the urban form factors and the LST. For example, a weak correlation is observed between the SVF and the LST, and no stable linear regression model can be established when the DIST is less than 250 m. However, after removing these samples, the correlation immediately increases.

In this study, the water bodies not only have a lower temperature using remote sensing images but also exert their cooling effect in the surrounding area in the daytime during the summer. The water bodies' cooling effect shows a decreasing trend as the DIST increases. The water bodies have an insignificant influence on the surrounding areas that are farther than one kilometer. After considering the DIST, the R-square values of the single and multiple regression models between the urban form factors and the LST are all markedly improved, although the linear regression has an insufficient capacity to predict the LST.

This study also indicates that the cooling effect of water bodies on their surrounding areas should be carefully considered when analyzing the thermal environmental effects of the urban form factors, particularly in urban areas that are near or surrounded by large water bodies, and the sampling design should be carefully considered to reduce the impact of water bodies, thus, truly reveal the impact mechanism of urban construction on the thermal environment.

6. Limitation and future work

In this study, non-physical urban form factors, such as the population density, are not considered, and the influence of waste heat discharged from human activities on the relationship between the urban form factors and LST is not considered. Furthermore, this study only used remote sensing images acquired in the daytime during the summer. In fact, the influence of the water bodies' cooling effect on the thermal environment depends on both the air temperature gradient and wind direction (Gunawardena et al., 2017; Theeuwes et al., 2013), and the extracted LST from the thermal image is mainly retrieved from the sensible heat portion and cannot capture the conversion of shortwave radiation to the latent heat of evaporation. Conducting the same study using air temperature could perhaps obtain better results, and it is significant to compare the difference between air temperature, surface temperature and LST retrieved from remote sensing images in future studies. In addition, many studies have shown that water bodies warm the city during nighttime or winter (Chun & Guhathakurta, 2017; Moyer & Hawkins, 2017; Steeneveld et al., 2014), which has a very different thermal environmental effect than that during the daytime in summer; whether a cooling effect or warming effect exists during nighttime or winter and influences the relationship between temperature and the urban form factors remains to be further studied.

The current study is based on the Chongqing city in China. In the future work, it is necessary to carry out a comparative study between different latitudes and different forms of cities, determine whether the cooling or warming effect of water bodies is influenced by urban form and climatic conditions. In addition, more studies are needed to optimize the urban form and improve the capacity of water bodies to mitigate urban heat islands in urban planning and design.

Acknowledgments

This study was supported by the National Natural Science Foundation of China (Grant No. 51778077). We thank three reviewers for their constructive comments and suggestions on the manuscript.

References

Alobaydi, D., Bakarman, M. A., & Obeidat, B. (2016). The impact of urban form configuration on the urban heat island: The case study of Baghdad, Iraq. *International conference on sustainable design, engineering and construction, 145*, 820–827.

Bokaie, M., Zarkesh, M. K., Arasteh, P. D., & Hosseini, A. (2016). Assessment of urban heat island based on the relationship between land surface temperature and land use/land cover in Tehran. *Sustainable Cities & Society, 23*, 94–104.

Chan, E. Y. Y., Goggins, W. B., Kim, J. J., & Griffiths, S. M. (2012). A study of intracity variation of temperature-related mortality and socioeconomic status among the Chinese population in Hong Kong. *Journal of Epidemiology and Community Health, 66*(4), 322–327.

Chen, X., & Zhang, Y. (2017). Impacts of urban surface characteristics on spatiotemporal pattern of land surface temperature in Kunming of China. *Sustainable Cities & Society, 32*, 87–99.

Chen, X. L., Zhao, H. M., Li, P. X., & Yin, Z. Y. (2006). Remote sensing image-based analysis of the relationship between urban heat island and land use/cover changes. *Remote Sensing of Environment, 104*(2), 133–146.

Chen, L., Ng, E., An, X., Ren, C., Lee, M., Wang, U., & He, Z. (2012). Sky view factor analysis of street canyons and its implications for daytime intra-urban air temperature differentials in high-rise, high-density urban areas of Hong Kong: A gis-based simulation approach. *International Journal of Climatology, 32*(1), 121–136.

Chen, Z., Jiang, W. G., Tang, Z. H., & Jia, K. (2016). Spatial-temporal pattern of vegetation index change and the relationship to land surface temperature in zoige. *ISPRS – international archives of the photogrammetry, remote sensing and spatial information sciences, XLI-B3,* 849–852.

Chen, A., Zhao, X., Yao, L., & Chen, L. (2016). Application of a new integrated landscape index to predict potential urban heat islands. *Ecological Indicators, 69*, 828–835.

Chun, B., & Guhathakurta, S. (2017). Daytime and nighttime urban heat islands statistical models for Atlanta. *Environment and Planning B: Urban Analytics and City Science, 44*(2), 308–327.

Chun, B., & Guldmann, J. M. (2014). Spatial statistical analysis and simulation of the urban heat island in high-density central cities. *Landscape & Urban Planning, 125*(3), 76–88.

Corburn, J. (2009). Cities, climate change and urban heat island mitigation: Localising global environmental science. *Urban Studies, 46*(2), 413–427.

Coutts, A. M., Tapper, N. J., Beringer, J., Loughnan, M., & Demuzere, M. (2013). Watering our cities: The capacity for water sensitive urban design to support urban cooling and improve human thermal comfort in the Australian context. *Progress in Physical Geography, 37*(1), 2–28.

Du, H., Song, X., Jiang, H., Kan, Z., Wang, Z., & Cai, Y. (2016). Research on the cooling island effects of water body: A case study of Shanghai China. *Ecological Indicators, 67*, 31–38.

Fouillet, A., Rey, G., Laurent, F., Pavillon, G., Bellec, S., Guihenneucjouyaux, C., et al. (2006). Excess mortality related to the August 2003 heat wave in France. *International Archives of Occupational & Environmental Health, 80*(1), 16–24.

Ganeshan, M., Murtugudde, R., & Imhoff, M. L. (2013). A multi-city analysis of the uhi-influence on warm season rainfall. *Urban Climate, 6*(6), 1–23.

Golany, G. S. (1996). Urban design morphology and thermal performance. *Atmospheric Environment, 30*(3), 455–465.

Gunawardena, K. R., Wells, M. J., & Kershaw, T. (2017). Utilising green and bluespace to mitigate urban heat island intensity. *Science of the Total Environment, 1040*, 584–585.

Guo, G., Wu, Z., Xiao, R., Chen, Y., Liu, X., & Zhang, X. (2015). Impacts of urban biophysical composition on land surface temperature in urban heat island clusters. *Landscape & Urban Planning, 135*, 1–10.

Guo, G., Zhou, X., Wu, Z., Xiao, R., & Chen, Y. (2016). Characterizing the impact of urban morphology heterogeneity on land surface temperature in Guangzhou: China. *Environmental Modelling & Software, 84*, 427–439.

Han, G. F., Cai, Z., Xie, Y. S., & Zeng, W. (2016). Correlation between urban construction and urban heat island: A case study in Kaizhou District, Chongqing. *Journal of Civil, Architectural & Environmental Engineering, 38*(5), 138–147. http://dx.doi.org/10.11835/j.issn.1674-4764.2016.05.018.

Hannah, D. M., Malcolm, I. A., Chris, S., & Youngson, A. F. (2010). Heat exchanges and temperatures within a salmon spawning stream in the cairngorms, scotland: Seasonal and sub-seasonal dynamics. *River Research & Applications, 20*(6), 635–652.

Hathway, E. A., & Sharples, S. (2012). The interaction of rivers and urban form in mitigating the urban heat island effect: A UK case study. *Building & Environment, 58*(58), 14–22.

Howard, L. (1818). *The climate of London, Vol. 1* W. Phillips, sold also by J. and A. Arch.

Huang, L., Zhao, D., Wang, J., Zhu, J., & Li, J. (2008). Scale impacts of land cover and vegetation corridors on urban thermal behavior in Nanjing, China. *Theoretical & Applied Climatology, 94*(3–4), 241–257.

Ichinose, T., Shimodozono, K., & Hanaki, K. (1999). Impact of anthropogenic heat on urban climate in Tokyo. *Atmospheric Environment, 33*(24–25), 3897–3909.

Kim, Y. H., Ryoo, S. B., Baik, J. J., Park, I. S., Koo, H. J., & Nam, J. C. (2008). Does the restoration of an inner-city stream in Seoul affect local thermal environment? *Theoretical & Applied Climatology, 92*(3–4), 239–248.

Klok, L., Zwart, S., Verhagen, H., & Mauri, E. (2012). The surface heat island of rotterdam and its relationship with urban surface characteristics. *Resources Conservation & Recycling, 64*(7), 23–29.

Lee, D., & Oh, K. (2017). Classifying urban climate zones (uczs) based on statistical analyses. *Urban Climate*. http://dx.doi.org/10.1016/j.uclim.2017.06.005 [in press].

Li, C., & Yu, C. W. (2014). Mitigation of urban heat development by cool island effect of green space and water body. *Lecture Notes in Electrical Engineering, 261*, 551–561.

Lin, P., Siu, S., Qin, H., & Gou, Z. (2017). Effects of urban planning indicators on urban heat island: A case study of pocket parks in high-rise high-density environment. *Landscape & Urban Planning, 168*(July), 48–60.

Masson, V., Marchadier, C., Adolphe, L., Aguejdad, R., Avner, P., Bonhomme, M., et al. (2014). Adapting cities to climate change: A systemic modelling approach. *Urban Climate, 10*(2), 407–429.

Matuschek, O., & Matzarakis, A. (2010). *Estimation of sky view factor in complex environment as a tool for applied climatological studies*, *20*, 534–539.

Middel, A., Häb, K., Brazel, A. J., Martin, C. A., & Guhathakurta, S. (2014). Impact of urban form and design on mid-afternoon microclimate in phoenix local climate zones. *Landscape & Urban Planning, 122*(2), 16–28.

Moyer, A. N., & Hawkins, T. W. (2017). River effects on the heat island of a small urban area. *Urban Climate, 21*, 262–277.

Murakawa, S., Sekine, T., Narita, K. I., & Nishina, D. (1991). Study of the effects of a river on the thermal environment in an urban area. *Energy and Buildings, 16*(3), 993–1001.

Nassar, A. K., Blackburn, G. A., & Whyatt, J. D. (2016). Dynamics and controls of urban heat sink and island phenomena in a desert city: Development of a local climate zone scheme using remotely-sensed inputs. *International Journal of Applied Earth Observation & Geoinformation, 51*, 76–90.

Ng, E., Yuan, C., Chen, L., Ren, C., & Fung, J. C. H. (2011). Improving the wind environment in high-density cities by understanding urban morphology and surface roughness: A study in Hong Kong. *Landscape & Urban Planning, 101*(1), 59–74.

Nichol, J. E., Fung, W. Y., Lam, K. S., & Wong, M. S. (2009). Urban heat island diagnosis using ASTER satellite images and 'in situ'air temperature. *Atmospheric Research, 94*(2), 276–284.

Nie, Q., & Xu, J. (2015). Understanding the effects of the impervious surfaces pattern on land surface temperature in an urban area. *Frontiers of Earth Science, 9*(2), 276–285.

Oke, T. R. (1974). *Review of urban climatology.* 1968–1973.

Oke, T. R. (1987). Boundary layer climates. *Earth Science Reviews, 27*(3) 265-265.

Santamouris, M. (2015). Analyzing the heat island magnitude and characteristics in one hundred Asian and Australian cities and regions. *Science of the Total Environment, 512-513*, 582–598.

Schwarz, N., & Manceur, A. M. (2014). Analyzing the influence of urban forms on surface urban heat islands in Europe. *Journal of Urban Planning & Development, 141*(3), A4014003.

Sobrino, J. A., Jiménez-Muñoz, J. C., & Paolini, L. (2004). Land surface temperature retrieval from landsat tm 5. *Remote Sensing of Environment, 90*(4), 434–440.

Steeneveld, G. J., Koopmans, S., Heusinkveld, B. G., & Theeuwes, N. E. (2014). Refreshing the role of open water surfaces on mitigating the maximum urban heat island effect. *Landscape & Urban Planning, 121*(1), 92–96.

Stewart, I. D., & Oke, T. R. (2012). Local climate zones for urban temperature studies. *Bulletin of the American Meteorological Society, 93*(12), 1879–1900.

Stewart, I. D. (2011). A systematic review and scientific critique of methodology in modern urban heat island literature. *International Journal of Climatology, 31*(2), 200–217.

Sun, R., Chen, A., Chen, L., & Lü, Y. (2012). Cooling effects of wetlands in an urban region: The case of beijing. *Ecological Indicators, 20*(9), 57–64.

Sun, R. (2012). How can urban water bodies be designed for climate adaptation? *Landscape & Urban Planning, 105*(1–2), 27–33.

Syafii, N. I., Ichinose, M., Kumakura, E., Jusuf, S. K., Chigusa, K., & Wong, N. H. (2017). Thermal environment assessment around bodies of water in urban canyons: A scale model study. *Sustainable Cities & Society, 34*, 79–89.

Takkanon, P. (2017). Uhi and thermal performance of office buildings in Bangkok. *Procedia Engineering, 180*, 241–251.

Taleghani, M., Kleerekoper, L., Tenpierik, M., & Dobbelsteen, A. V. D. (2015). Outdoor thermal comfort within five different urban forms in The Netherlands. *Building & Environment, 83*, 65–78.

Theeuwes, N. E., Solcerová, A., & Steeneveld, G. J. (2013). Modeling the influence of open water surfaces on the summertime temperature and thermal comfort in the city. *Journal of Geophysical Research Atmospheres, 118*(16), 8881–8896.

United Nations, Department of Economic and social Affairs (UN-DESA) (2010). *World urbanization prospects: The 2009 revision.* http://esa.un.org/unpd/wup/index.htm.

Völker, S., Baumeister, H., Claßen, T., Hornberg, C., & Kistemann, T. (2013). Evidence for the temperature-mitigating capacity of urban blue space—A health geographic perspective. *Erdkunde, 67*(4), 355–371.

Watson, I. D., & Johnson, G. T. (1987). Graphical estimation of sky view-factors in urban environments. *Journal of Climatology, 7*(2), 193–197.

Wong, N. H., Jusuf, S. K., Syafii, N. I., Chen, Y., Hajadi, N., Sathyanarayanan, H., et al. (2011). Evaluation of the impact of the surrounding urban morphology on building energy consumption. *Solar Energy, 85*(1), 57–71.

Wong, M. S., Nichol, J., & Ng, E. (2011). A study of the wall effect caused by proliferation of high-rise buildings using GIS techniques. *Landscape and Urban Planning, 102*(4), 245–253.

Xu, D., & Chen, R. (2017). Comparison of urban heat island and urban reflection in Nanjing City of China. *Sustainable Cities & Society, 31*, 26–36.

Xu, Y., Ren, C., Ma, P., Ho, J., Wang, W., Lau, K. L., et al. (2017). Urban morphology detection and computation for urban climate research. *Landscape & Urban Planning, 167*, 212–224.

Yang, L., Li, G., Lin, Y., & Ye, L. (2011). Progress and prospect on relationship research

between urban form and carbon emission. *Urban Studies, 18*(2), 12–17.
Yong, S. U., Wen, H. U., & Zhao, R. (2004). The ecological system design methods based on the dominant ecological gene in the urban hub: And the application in the urban hub of spb cq. *Urban Planning Forum, 5*, 008.
Yue, W., Xu, J., Tan, W., & Xu, L. (2007). The relationship between land surface temperature and NDVI with remote sensing: Application to Shanghai Landsat 7 ETM+ data. *International Journal of Remote Sensing, 28*(15), 3205–3226.
Zhang, X., Estoque, R. C., & Murayama, Y. (2017). An urban heat island study in Nanchang City, China based on land surface temperature and social-ecological variables. *Sustainable Cities & Society, 32*, 557–568.
Zhang, Y., Murray, A. T., & Ii, B. L. T. (2017). Optimizing green space locations to reduce daytime and nighttime urban heat island effects in Phoenix Arizona. *Landscape & Urban Planning, 165*, 162–171.
Zhao, C., Fu, G., Liu, X., & Fu, F. (2011). Urban planning indicators, morphology and climate indicators: A case study for a north-south transect of Beijing, China. *Building & Environment, 46*(5), 1174–1183.